11-2022

MODIFIED TITANI DERIVED FROM TI – OXO CLUSTERS: SYNTHESIS, STRUCTURE, AND PHOTOCATALYTIC ACTIVITY

Fatmah Rashed Ali Alkindi

MASTER THESIS NO. 2022: 78

College of Science

Department of Chemistry

MODIFIED TITANI DERIVED FROM TI – OXO CLUSTERS: SYNTHESIS, STRUCTURE, AND PHOTOCATALYTIC ACTIVITY

Fatmah Rashed Ali Alkindi

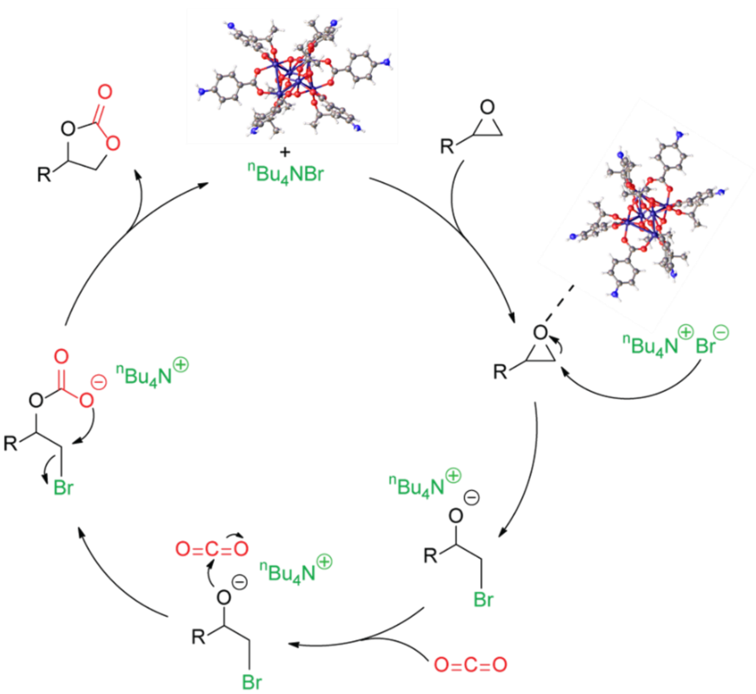

November 2022

United Arab Emirates University

College of Science

Department of Chemistry

MODIFIED TITANI DERIVED FROM TI – OXO CLUSTERS: SYNTHESIS, STRUCTURE, AND PHOTOCATALYTIC ACTIVITY

Fatmah Rashed Ali Alkindi

This thesis is submitted in partial fulfilment of the requirements for the degree of Master of Science in Chemistry

November 2022

United Arab Emirates University Master Thesis
2022: 78

Cover: Plausible mechanism for CO_2 cycloaddition of epoxides to cyclic carbonates

(Photo: By Fatmah Rashed Ali Alkindi)

Print: University Print Service, UAEU 2022

Declaration of Original Work

I, Fatmah Rashed Ali Alkindi, the undersigned, a graduate student at the United Arab Emirates University (UAEU), and the author of this thesis entitled “*Modified Titani derived from Ti – Oxo Clusters: Synthesis, Structure, and Photocatalytic Activity*”, hereby, solemnly declare that this is the original research work done by me under the supervision of Dr. Ahmed H. Alzamly, in the College of Science at UAEU. This work has not previously formed the basis for the award of any academic degree, diploma or a similar title at this or any other university. Any materials borrowed from other sources (whether published or unpublished) and relied upon or included in my thesis have been properly cited and acknowledged in accordance with appropriate academic conventions. I further declare that there is no potential conflict of interest with respect to the research, data collection, authorship, presentation and/or publication of this thesis.

Student’s Signature: ________________

Date: ___12/12/2022_____

Approval of the Master Thesis

This Master Thesis is approved by the following Examining Committee Members:

1) Advisor (Committee Chair): Ahmed H. Alzamly

   Title: Associate Professor

   Department of Chemistry

   College of Science

   Signature ______________________ Date 27/12/2022

2) Member: Na'il Saleh

   Title: Professor

   Department of Chemistry

   College of Science

   Signature ______________________ Date 27/12/2022

3) Member (External Examiner): Ihsan Ahmed Shehadi

   Title: Associate Professor

   Department of Chemistry

   Institution: Sharjah University, UAE

   Signature ______________________ Date 27/12/2022

This Master Thesis is accepted by:

Dean of the College of Science: Professor Maamar Benkraouda

Signature Maamar Benkraouda

Date Jan. 3, 2023

Dean of the College of Graduate Studies: Professor Ali Al-Marzouqi

Signature Ali Hassan

Date January 3, 2023

Abstract

Titanium dioxide (TiO_2), an important semiconductor, has been used in various applications ranging from sunblock additives to self-cleaning window coatings, antibacterial agents, photovoltaics, and photocatalysis. Due to its photostability, TiO_2 is an extensively used semiconductor photocatalyst in many industries. This thesis represents the synthesis, structure, and photocatalytic activity of TiO_2 (Anatase) photocatalyst, which was prepared using hexanuclear titanium-oxo cluster precursor via temperature-controlled calcination. The optical property of the prepared photocatalyst was investigated using UV-Vis diffuse reflectance spectroscopy (UV-Vis DRS), powder X-ray diffraction (PXRD) for phase determination, scanning electron microscopy (SEM) for morphology and structural analysis, Brunauer−Emmett−Teller (BET) for the specific surface area and porosity determination, and energy-dispersive X-ray spectroscopy (EDX) for elemental chemical identification. Photocatalytic activities of the as-prepared TiO_2 were evaluated using cycloaddition reaction of different epoxides to CO_2. As prepared, TiO_2 (anatase) quantitatively achieved cyclic carbonates formation over a range of epoxides used for CO_2 cycloaddition reaction.

Keywords: Titanium oxo cluster, TiO_2, band gap, Photocatalyst, cycloaddition.

Title and Abstract (in Arabic)

تحضير، دراسة هيكل و نشاط المحفز الضوئي لثاني أكسيد التيتانيوم (Anatase) الذي تم تحضيره باستخدام (Ti-Oxo-Cluster)

الملخص

يعتبر ثاني أكسيد التيتانيوم (TiO_2) من المواد أشباه الموصلات المهمة التي تتمتع بالعديد من الخصائص والتي يتم استخدامها في عدة تطبيقات مثل أوقية الشمس، طلاء النوافذ ذاتية التنظيف وكعوامل مضادة للبكتيريا والخلايا الكهروضوئية، بالإضافة إلى التحفيز الضوئي. نظرا لاستقراره الضوئي, يستخدم ثاني أكسيد التيتانيوم على نطاق واسع من الصناعات. تعرض هذه الأطروحة طريقة تحضير، دراسة هيكل و نشاط المحفز الضوئي لثاني أكسيد التيتانيوم (Anatase) الذي تم تحضيره باستخدام (Ti-oxo-cluster) من خلال تكليسه بالتحكم بدرجات الحرارة. تم تحديد نطاق نشاط المحفز الضوئي المحضر عن طريق استخدام التحليل الطيفي للإنعكاس المنتشر (UV-VIS DRS), حيود المسحوق بالأشعة السينية (PXRD) لتحديد البنية البلورية،المسح المجهري الإلكتروني (SEM) للتشكيل و التحليل الهيكلي ، بالإضافة إلى نظرية برونور-إيميت-تيلر (BET) لتحديد مساحة السطح و المسامية ، و الطيف الطيفي للأشعة السينية المشتتة للطاقة (EDX) لتحديد العناصر الكيميائية. تم تقييم نشاط المحفز (TiO_2) الضوئي من خلال دراسة تفاعل الإضافة الحلقية الضوئي (cycloaddition) لإيبوكسيدات مختلفة مع ثاني أكسيد الكربون. حقق ثاني أكسيد التيتانيوم (TiO_2) المحضر نجاحاً في تكوين مركبات كربونات حلقية باستخدام مجموعة من الإيبوكسايدات المستخدمة في تفاعل الإضافة الضوئي (cycloaddition) لثاني أكسيد الكربون.

مفاهيم البحث الرئيسية: ثاني أكسيد التيتانيوم،التحفيز الضوئي، تفاعل الإضافة الضوئي، ثاني أكسيد الكربون.

Acknowledgements

First and foremost, my praise and appreciation to God, the Almighty, for His showers of blessings during my studies, which enabled me to complete this research successfully.

I would like to acknowledge my supervisor, Dr. Ahmed H. Alzamly, for giving me the chance to do research and offering vital assistance during this process. His energy, vision, genuineness, and determination have all left an indelible impression on me. He taught me the approach to conducting research and presenting the findings as simply as possible. Working and studying under his supervision was an incredible honor and pleasure. I am deeply appreciative of all he has provided for me.

I am eternally thankful to my beloved father Rashed Alkindi, who supported and believed in me, as well as my incredible, exceptional, and loving mother, for their unwavering support. I appreciate your affection and efforts to help me become a better person. Because of your prayers and wise advice, I have accomplished much.

I would like to express my sincere gratitude to my sister Shama, who, throughout the years, has provided me with invaluable support and amusement. Thank you for always being cheerful.

I owe a great deal to my friends Reem and Lamia, who supported me and stood by me during this journey. Thank you for always being the compassionate, kind, and giving friends I wished for. I am so thankful to have you in my life

Dedication

To my beloved parents and family

Table of Contents

List of Tables

List of Figures

Chapter 1: Introduction

Throughout the world, people's lives are at risk due to pollution and climate change. Because of the rapid economic development and the growing population, environmental and energy issues have received a great deal of attention.[1] Artificial photosynthetic systems using cheap heterogenous photocatalysts might be the most promising solution to these problems.[2] Photocatalytic water splitting and CO_2 reduction are used to mimic natural photosynthesis, it would be ideal for creating a single material that serves as an ideal platform by combining photosensitizers and catalytic centers in a single crystalline lattice.[3,4]

There are many uses for titanium dioxide (TiO_2), including photocatalysis,[5] paints, cosmetics,[6] removal of water and air pollutants,[7] photodegradation of organic contanimants,[8] and dye-sensitized solar cells (DSSCs) based materials.[9] Its unique optical properties, low price, lack of toxicity, and wide availability all play a role. Both the band gap and the visible-light photocatalytic performance of TiO_2 are significantly subpar.[10,11] However, numerous methods, from structural modulation to metal incorporation, have been developed to boost inefficient photocatalytic performance. The photocatalytic activity of TiO_2 is highly sensitive to its crystal structure, particle size, surface area, and the raw materials from which the catalyst is derived. Preparation methods have been found to have a significant impact on nanocrystalline TiO_2's physical and chemical properties.[12]

The preparation technique substantially affects titanium dioxide's physical and chemical properties.[13] Hydro/solvothermal or sol-gel methods are often used to synthesize TiO_2. Using hydrothermal processes has some drawbacks, including slow reaction durations, the impact of alkaline concentration, difficulty monitoring crystal growth, temperature effects, and the production of unstable materials.[14] But unlike the solvothermal method, organic solvents can produce anions-free products and have reduced permittivity, allowing for partial particle ionization.[5] Unfortunately, there are certain drawbacks to the sol-gel method, such as a protracted drying procedure, considerable volume loss, cracking while drying, and relatively costly precursor pricing.[15] However, it allows for exceptional control over material composition and purity.[16]

When exposed to UV irradiation, Ti-oxo-cluster has been shown to have a remarkable capacity for UV absorption and significant activity for CO_2 fixation.[17] This makes it one of the many molecular metal–oxo clusters materials employed as photocatalysts. Because of their various beneficial features, molecular metal–oxo clusters make excellent adsorbents. The amorphization process does not affect the sorption capabilities of these molecular materials, enabling them to be utilized in a range of settings, including those that involve moist air. Second, because of these materials' intrinsic discreteness and solubility, they are ideally suited for processing techniques that include either solids or solutions. In addition, metal oxo-clusters can be quickly produced and exhibit a large variety of structural diversities. This is because they feature a broad range of oxidation states. The high propensity of early transition metals like titanium (IV) and oxo-bridged multinuclear clusters produced from these is encouraging by the sense of the discovery of novel molecular solids with even more fascinating features.[18]

Because of its abundance, lack of toxicity, and inflammability, carbon dioxide (CO_2) can be used as a C1 feedstock despite being both cheap and renewable.[19] Academics have sought viable strategies to recycle it into long-lasting and practical items. Due to its efficiency as an atom economy process, CO_2 cycloaddition to epoxides is among the most highly profitable methods in sustainable advancement, such as pharmaceuticals and high-value chemicals.[20] There are several applications for cyclic carbonates, including electrolytes in lithium-ion batteries,[21] polar aprotic solvents for organic reactions,[22] monomers in the production of polycarbonate, and intermediates in the biomedical and pharmaceutical fields,[23,24] The output of disinfectants and herbicides also necessitates the use of cyclic carbonates.[25]

For more than 50 years, it has been known that cyclic carbonates (CCs) can be made by inserting carbon dioxide (CO_2) into epoxides. An important example is propylene carbonate (PC), which serves as a feedstock alongside unsaturated cyclo-carbonates and as a green dipolar aprotic solvent for organic synthesis as an alternative to the harmful propylene oxide (PO).[26] Poly (propylene carbonate) (PPC) also has excellent compatibility with other materials used in the medical field, and it degrades quickly.[5] Commonly used harmful organic solvents, including tetrahydrofuran, chloroform, and aromatic solvents, can be replaced with CCs because they are safer and better for the environment.[27]

In this thesis, we describe the controlled synthesis of an anatase TiO_2 polymorph from a hexanuclear titanium oxo cluster. The cycloaddition reaction of epoxide to CO_2 under simulated UV/Visible light irradiation was used to assess the photocatalyst's performance. In addition, a titanium (IV)-oxo carboxylate cluster was prepared in 2-propanol using titanium (IV) isopropoxide and 4-aminobenzoic acid. Its photocatalytic investigation of CO_2 cycloaddition to epoxides is presented.

Chapter 2: Photocatalytic Cyclic Carbonates Formation over Hexanuclear Titanium-Oxo Cluster under Simulated Visible Light Irradiation

2.1 Introduction

Photocatalyst research has surged in recent years for many purposes such as purification of air and water,[3,4] eliminating hazardous waste,[29] and producing clean energy.[30] Hydrogen can be produced as a clean energy source via photocatalytic hydrogen production from water, which has received significant attention.[31,32] Moreover, photocatalysts have also been studied for organic transformations as an environment-friendly method of pursuing green chemistry.[33,34]

Due to the fact that most photocatalysts respond only to ultraviolet light,[35] only ~ 5% of the solar energy reaching the earth is converted into useful energy.[36,37] As a result of this limited potential, the development of an effective photocatalyst for converting energy from the sun into chemical energy is a critical research field regarding the use of abundant light sources.[38]

There has been a significantly attention in titanium oxo-clusters (TOCs) in recent years due to their similar photocatalytic properties to TiO_2.[39] Numerous TOCs and their derivatives have been reported during the past decade, yet there has been relatively little systematic research on how they affect their photocatalytic activity and bandgaps.[40] A visible-light-responsive TOCs photocatalysts has been developed,[41] however, photocatalytic activity needs to be improved and the use of TOCs photocatalysts for other reactions as well as organic transformations should be explored.

It is important to acknowledge, however, that the main disadvantages of TOC such as wide bandgaps,[42] poor light absorption,[40] and rapid charge recombination[43] have greatly hindered the broad application of TOC in solar-driven reactions on a large scale. As a result, it is extremely crucial that TOC-based catalysts are sensitive to visible light.

Here, we report titanium (IV)−oxo carboxylate cluster[18] and made from titanium (IV) isopropoxide and excess of 4-aminobenzoic acid in 2-propanol. Its photocatalytic study toward cycloaddition of CO_2 to epoxides is presented.

2.2 Experimental

2.2.1 Materials

Titanium (IV) isopropoxide, 2-propanol (i-PrOH, 99.7%), 4-aminobenzoic acid ($C_7H_7NO_2$), $^nBu_4NBr$ (TBAB), acetonitrile (ACN) and methanol (MeOH), were obtained from Sigma Aldrich and used as is.

2.2.2 Hexanuclear Titanium Oxo Cluster Synthesis

Using a previously published method with slight modification, in a sealed tube, 4-aminobenzoic acid (1152.6 mg, 8.4 mmol) was dissolved in 60 mL isopropanol, followed by addition of titanium (IV) isopropoxide (621.6 mL, 2.1 mmol). After sealing the tube, it was heated at 100°C for 72 hours. After filtering and washing with excess isopropanol, the yellow crystals were dried under vacuum for an hour.

2.3 Characterization

2.3.1 Powder X-Ray Diffraction (PXRD)

Powder X-ray diffraction (PXRD) was measured on a Rigaku MiniFlex benchtop X-ray diffractometer assembled with a CuK radiation tube (λ = 1.542 Å) operating at 40 kV at a rate of 2° min^{-1} over a range of 3–50° 2θ.

2.3.2 UV–Vis Diffuse Reflectance Spectroscopy (UV–Vis DRS)

Shimadzu UV-3600 UV–Vis diffuse reflectance spectrophotometer was used to measure the photocatalysts' band gap energies. Baseline correction was performed using barium sulfate ($BaSO_4$) in the 200-800 nm wavelength range. Tauc plots were used to calculate band gap energies.

2.3.3 Thermogravimetric Analysis (TGA)

Shimadzu TGA-50 analyser was used to conduct TGA under nitrogen flow at a rate of 100 mL min^{-1}. The chamber heating flow was 5°C min^{-1} where the activated Ln-MOF sample was placed in an aluminium pan holder.

2.3.4 Scanning Electron Microscopy (SEM)

Quattro ESEM, with a 30 kV accelerating voltage, was used to capture scanning electron microscopy (SEM) images in high vacuum. To analyze the EDX data, a Quattro ESEM with an EDX detector was used.

2.3.5 Nuclear Magnetic Resonance (NMR)

In order to confirm the formation of cyclic carbonates, ^{1}H-NMR spectra were analysed using Varian-400 MHz NMR instrument using chloroform-d as a solvent.

2.4 Photocatalytic Activity

The photocatalytic conversion of epoxides to cyclic carbonate was performed in 4 ml of acetonitrile and 1 ml of methanol, 9 mg of tetra butyl ammonium bromide ($^{n}Bu_4NBr$) as a co-catalyst, 10 mg of photocatalyst, 1.24 mmol of epoxides. The amount of CO_2 was 0.045 mole. The mixture was then poured into a 75 mL sealed tube. Mixture then stirred under a halogen lamp irradiation for 24 hours (300 W, brand name OSRAM HALOLINE). The product was obtained by syringe filtration, then extracted and analysed.

2.5 Results and Discussion

2.5.1 PXRD of Hexanuclear Titanium Oxo Cluster

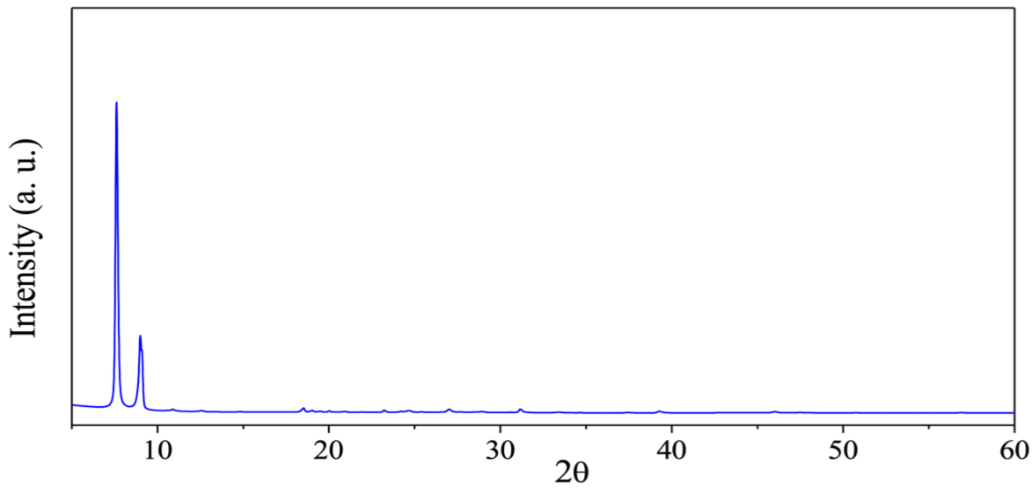

Figure 1: PXRD patterns of Titanium-Oxo cluster

Figure 1 represent PXRD patterns of synthesized titanium oxo cluster photocatalyst and the corresponding simulated spectrum. A lack of extra peaks related to impurities in the sample indicates the material is pure.

2.5.2 UV-Vis DRS of Hexanuclear Titanium Oxo Cluster

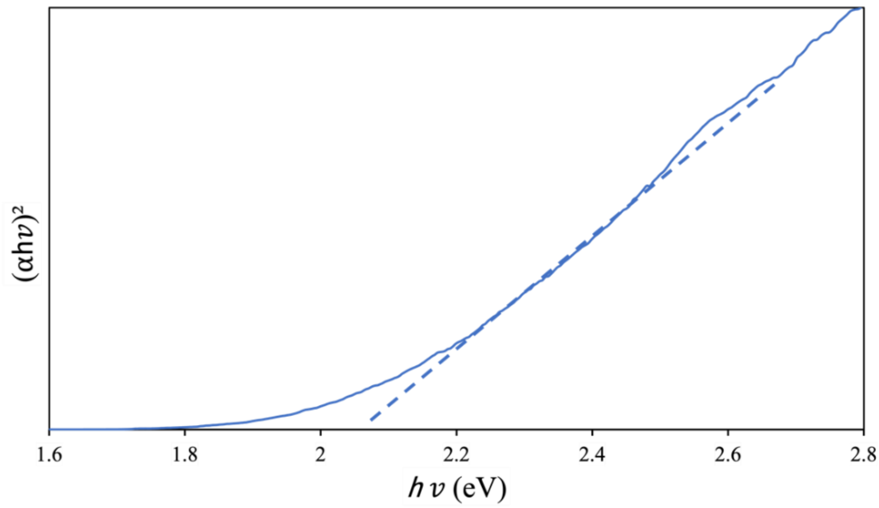

Figure 2: Tuac plot of Titanium-Oxo cluster

The UV-DRS analysis of titanium oxo cluster as-prepared photocatalyst is depicted by the Tuac plot in Figure 2. The sample absorbs a lot of UV-VIS light, which is typical of photoactive materials. Based on a direct allowed transition, the band gap in the pure prepared titanium oxo cluster was calculated to be 2.1 eV.

2.5.3 Thermogravimetric Analysis (TGA) of Hexanuclear Titanium Oxo Cluster

For titanium oxo cluster, weight loss profiles were measured using thermogravimetric analysis (TGA) (Figure 3). Around 10% weight loss was observed at 260–280°C which attributed due to loss of water molecules. Followed by a significant weight loss in the 280–500°C range of 66% because of the exothermic decomposition of the organic linker is observed in this range. The left mass is due to the formation of titanium oxide in the form of anatase, which degrades at higher temperatures.

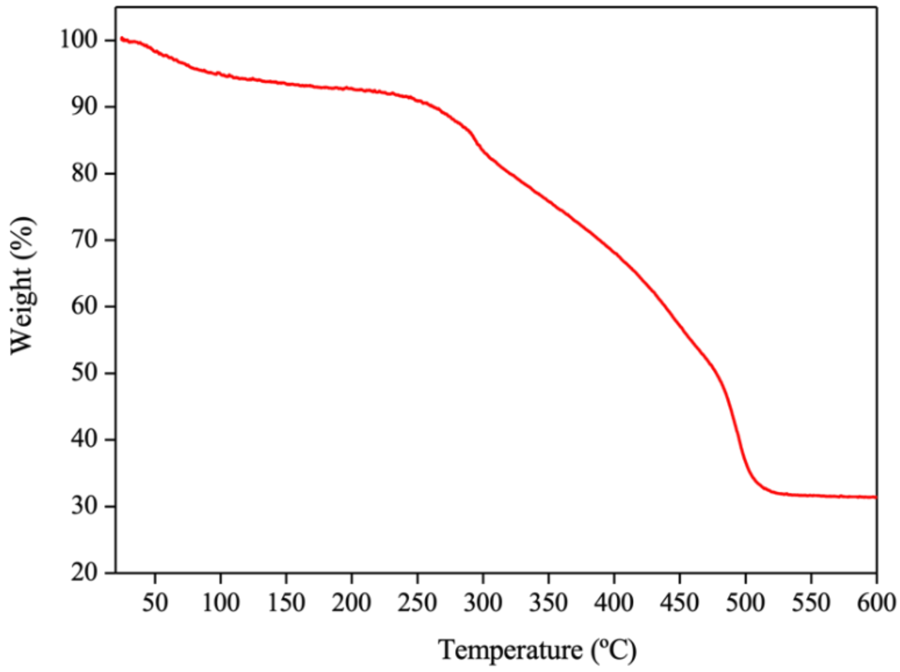

Figure 3: Thermogravimetric analysis of Titanium-Oxo cluster

2.5.4 Scanning Electron Microscopy

The surface morphology and the particle shape of Titanium-oxo Cluster is shown in Figure 4 at two different scale bars. The cluster has blocks of undefined morphology from rode-like to cubic-like crystals. These shapes were confirmed from the literature.

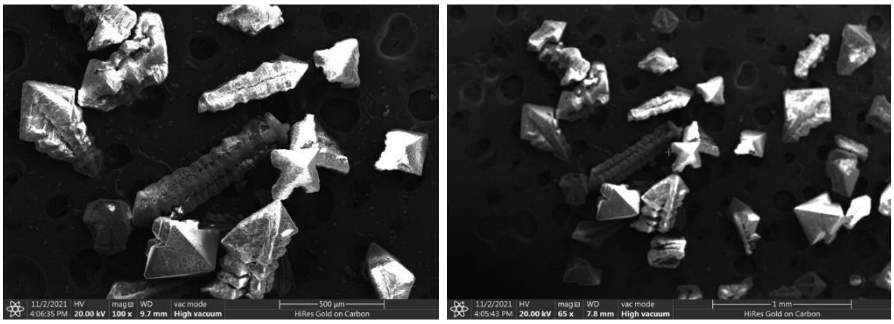

Figure 4: SEM images of Titanium-Oxo cluster

2.5.5 Photocatalytic Activities of Hexanuclear Titanium Oxo Cluster

The chemical shift of Ha protons in each epoxide relative to the cyclic carbonates formed Hb and their corresponding yields are shown in Table 1. The 1a, 1c and 1e represents propylene oxide, 2-(4-chlorophenyl) oxirane and 1,2-epoxy-3-phenoxypropane respectively.

Table 1: The chemical shift of Ha protons in each epoxide relative to the cyclic carbonates formed Hb and their corresponding yields

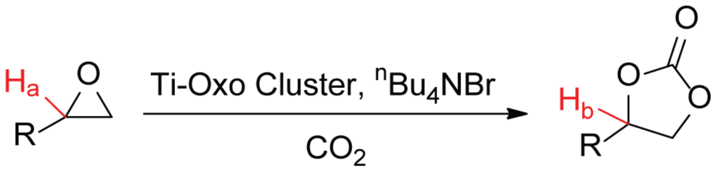

Epoxide	$^{\delta}H_a$ ($CDCl_3$)	$^{\delta}H_b$ ($CDCl_3$)	Product yield (%)	TON[c]	TOF (h^{-1})[d]
1a	2.98	4.85	99.9	59.54	2.48
1c	3.83	5.65	40	23.81	0.99
1e	3.04	4.70	55	32.74	1.36

[a] Reaction conditions: epoxide (1.429 mmol), photocatalyst (10 mg, 0.024mmol), $^nBu_4NBr$ (9 mg, 0.028 mmol) and 0.045 mmol carbon dioxide at 353 K and 24 h.
[b] Yield of isolated product was determined by ^1H NMR spectroscopy.
[c]TON= (mmols of product)/ (mmols of catalyst).
[d]TOF = (mmols of product)/ (mmols of catalyst) (reaction time, hour).

propylene oxide (1a), 2-(4-chlorophenyl) oxirane (1c) and 1,2-epoxy-3-phenoxypropane (1e)

2.6 NMR Spectra

Nuclear Magnetic Resonance of propylene oxide (1a), 2-(4-chlorophenyl) oxirane (1c) and 1,2-epoxy-3-phenoxypropane (1e) are illustrated in Figure 5.

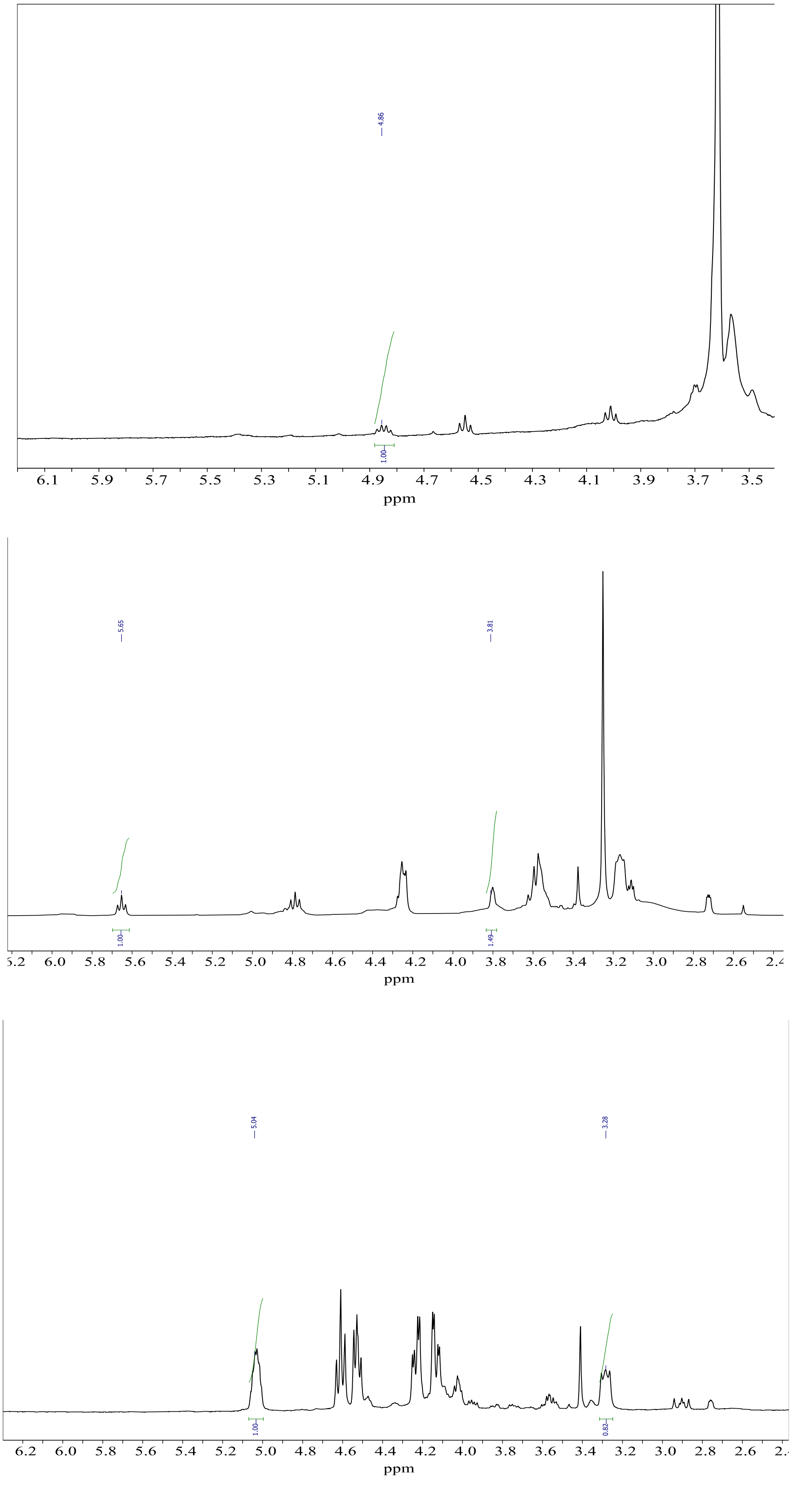

Figure 5: NMR of propylene oxide (1a), 2-(4-chlorophenyl) oxirane (1c) and 1,2-epoxy-3-phenoxypropane (1e)

The CO_2 cycloaddition reaction started when the at Lewis acid site (Ti^{3+} nodes) in prepared hexa-nuclear titanium oxo cluster coordinate with epoxides oxygen atom which resulted in weaking the carbon-oxygen bond. The C atom of the epoxide is then attacked by TBAB. Under light irradiation, CO_2 will be activated and attack the C in epoxides to produce the cyclic carbonate compound (Figure 6). The active Ti sites in titanium oxo cluster were crucial role in activating the cycloaddition reaction.

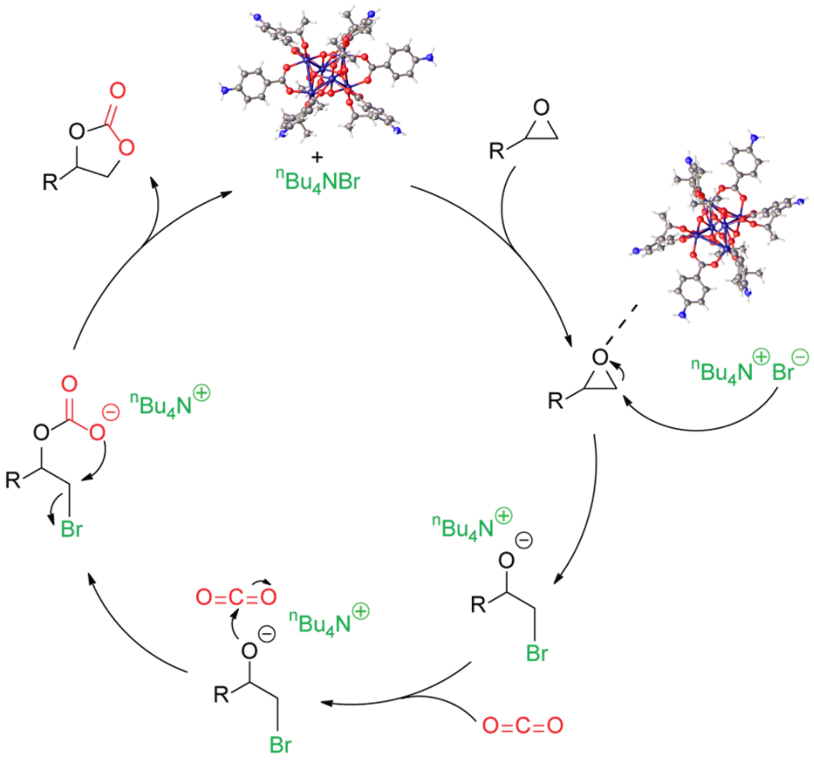

Figure 6: Plausible mechanism for CO_2 cycloaddition of epoxides to cyclic carbonates

2.7 Conclusion

Titanium-Oxo Cluster was utilized as an active photocatalyst in the CO_2 cycloaddition reaction of epoxides to cyclic carbonate due to its 2.1 eV ultraviolet band gaps. The optical properties of the prepared photocatalyst were investigated by means of DRS, PXRD and EM). Hexanuclear titanium oxo cluster, as a model photocatalytic cycloaddition reaction of CO_2 to epoxides, demonstrated a high conversion rate to the formation of cyclic carbonates.

Chapter 3: Anatase TiO_2 Derived from Hexanuclear Titanium-Oxo Cluster: Synthesis, Characterization, and Photocatalytic Activity

3.1 Introduction

An important semiconductor, titanium dioxide (TiO_2) has been used for various application spanning from additives in sunblock, coating of a self-cleaning windows, antibacterial agent, photovoltaics and photocatalysis.[44,45] The enhanced applicability of TiO_2 in the UV light is due to its wide band gap of ~3.03–3.3 eV, allowing excitation of electrons from valence band (oxygen, 2p) to the conduction band (titanium, 3d).[46] Due to its photostability, TiO_2 is extensively used semiconductor photocatalyst in many industries.[5,47,48] Nonetheless, the photocatalytic efficiency of TiO_2 decreases substantially due to the rapid recombination of photo-induced electrons (e^-) and holes (h^+) generated when TiO_2 surface irradiated with the ultraviolet (UV) light (~ 3.3 eV).[48,49] Among TiO_2 three major polymorphs: anatase, rutile and brookite, the anatase is the most active upon light irradiation due to its redox/surface properties and high surface area.[50,51] Nevertheless, heating either brookite or anatase to higher temperature results in formation of the most stable phase i.e., the rutile polymorph.[52]

There are many synthetic methods applied for the synthesis of TiO_2; hydro/solvothermal method[53,54] and sol-gel method[55,56] are among the most widely used. Hydrothermal method drawbacks include long synthesis time,[57] affected by alkaline concentration,[58] inability to monitor crystals growth,[59] temperature effect.[60] Above mentioned factors result in significant changes in morphology of the produced TiO_2 particles. though, Solvothermal method allows shape, and size control over hydrothermal method, on the other hand, organic solvent exhibit low permittivity allowing partial particle ionization,[60] moreover, the use of organic solvent during the solvothermal process results in a anions free product.[61]

Although Sol-gel method sounds very promising for synthesis of TiO_2 enable the use of low preparing temperature and compositional homogeneity at the molecular level.[62,63] The sol-gel method is widely used in synthesis of TiO_2 through an acid-catalyzed step of titanium (IV) alkoxides and produces powder of uniform size and shape. On the other hand, to obtain uniform nanoscale TiO_2, precise control of the hydrolysis step by adjusting the pH and temperature of the sol is critical. To this end, although the sol-gel method enables large-scale synthesis of high surface area TiO_2 nanoparticles, limitations such as particle aggregation and broad particle size distribution still exist.[64]

As a result of changes in the crystal size and textural qualities of nanostructured TiO_2, extensive research has recently been reported for the synthesis of nanostructured TiO_2 with diverse attributes for specific applications. From a synthetic perspective, it is clear that by modifying the current processes, it is still possible to create nanostructured TiO_2 particles with improved characteristics.

In this work, we present a controlled synthesis of anatase polymorph of TiO_2 derived from hexanuclear titanium oxo cluster. The performance of the photocatalyst was investigated using the cycloaddition reaction of epoxide to CO_2 as a model photocatalytic reaction.

3.2 Experimental

3.2.1 Materials

Titanium (IV) isopropoxide, 2-propanol (*i*-PrOH, 99.7%), 4-aminobenzoic acid ($C_7H_7NO_2$), $^{n}Bu_4NBr$ (TBAB), acetonitrile (ACN), dichloromethane (DCM), and methanol (MeOH), were secured from Sigma Aldrich and used as received.

3.2.2 Synthesis of Hexanuclear Titanium Oxo Cluster and Anatase TiO_2

Titanium oxo cluster was synthesized as previously reported with minor modification.[18] Typically, in a sealed glass tube, 1.2g (8.4 mmol) of 4-aminobenzoic acid was solubilized in 60 mL isopropanol, 0.6 mL (2.1 mmol) of titanium (IV) isopropoxide was then added under constant stirring. The tube was sealed and positioned in a preheated oven at 100°C for three days. The resulted yellow crystals were filtered, then washed with isopropanol, then dried under vacuum for 1 hour. The synthesized Titanium oxo cluster was subjected to calcination at 500°C for 5 hours to obtain anatase TiO_2.

3.3 Characterization

3.3.1 Powder X-Ray Diffraction (PXRD)

Detailed instrument description was outlined in chapter 2.

3.3.2 UV–Vis Diffuse Reflectance Spectroscopy (UV–Vis DRS)

Detailed instrument description was outlined in chapter 2. Tauc plot method was applied for band gap energy calculation.[65]

3.3.3 N_2 Adsorption–Desorption Analysis

Surface area and porosity were determined using nitrogen adsorption–desorption curve performed at 77 K. Sample was placed under vacuum at 150°C for 2 hours preceding analysis. Brunauer–Emmett–Teller (BET) method was used to calculate the surface area.

3.3.4 Scanning Electron Microscopy (SEM) and Energy-Dispersive X-Ray Spectroscopy (EDX)

Detailed instrument description was outlined in chapter 2.

3.3.5 Nuclear Magnetic Resonance (NMR)

Detailed instrument description was outlined in chapter 2.

3.4 Photocatalytic Activity

The photocatalytic cycloaddition of epoxides to carbon dioxides was performed in 4 mL of acetonitrile and 1mL methanol. To the reaction mixture, 9 mg of tetra butyl ammonium bromide ($^{n}Bu_4NBr$) as a co-catalyst, 10 mg TiO_2 photocatalyst, 1.24 mmol epoxides, and 0.045 mol of CO_2 were added to a 75 mL sealed tube and stirred for 24 hours under a halogen lamp irradiation (300 W, OSRAM HALOLINE). Solubility of CO_2 in the mixture was improved by using acetonitrile as a solvent. However, methanol is a hole-scavenger in photoreactions. After reaction is complete, excess CO_2 was degassed, cyclic carbonate was extracted using CH_2Cl_2 and then characterized.

3.5 Results and Discussion

3.5.1 PXRD Analysis of Pure Anatase-Phase TiO_2

Figure 7 displays PXRD patterns of synthesized photocatalysts; both the titanium oxo cluster and corresponding anatase TiO_2. As shown below, the PXRD of the prepared titanium oxo cluster is in perfect agreement with the PXRD of the previously reported.[24] Moreover, the PXRD database (JCPDS file No. 21-1272)[66] showed that all diffraction peaks were correctly indexed to those of the pure tetragonal phases of TiO_2 (anatase). No extra peaks associated with starting materials, or any impurities were observed indicating successful preparation of pure anatase-phase TiO_2.

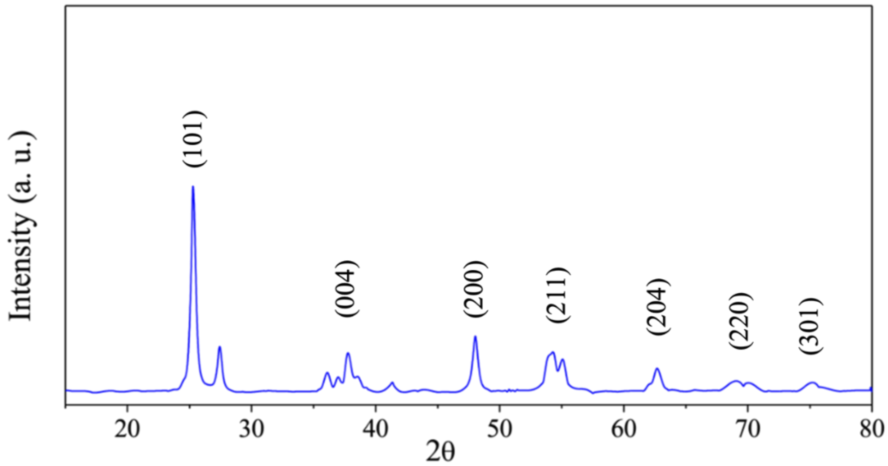

Figure 7: PXRD pattern of pure anatase-phase TiO_2

3.5.2 UV-Vis DRS of Pure Anatase-Phase TiO_2

The UV-DRS analysis of the as-prepared TiO_2 photocatalyst was calculated using Tauc plot shown in Figure 8. The photocatalyst exhibits a strong absorption in the UV-Vis region of the spectrum which as might be expected for TiO_2 materials.[46] Based on a direct allowed transition, the band gap was calculated to be 3.1 eV for as-prepared pure anatase-phase TiO_2.

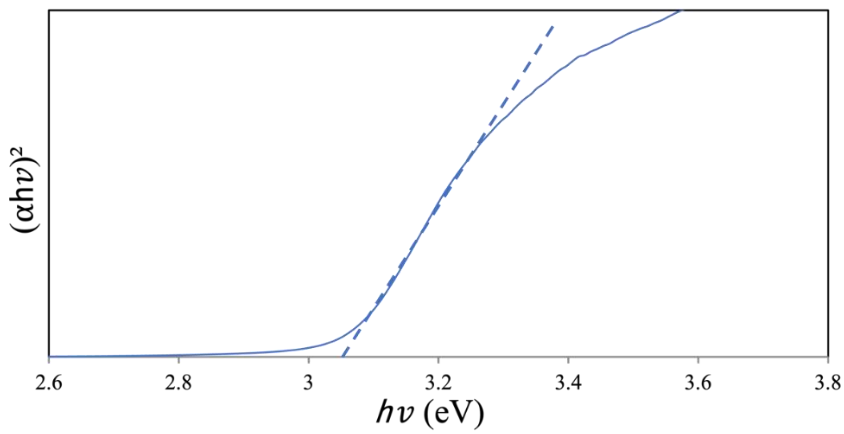

Figure 8: Band gap energy of pure anatase-phase TiO_2

3.5.3 N_2 Adsorption–Desorption Analyses of Pure Anatase-Phase TiO_2

N_2 adsorption-desorption isotherm of pure TiO_2 is shown in Figure 9. The as-prepared pure anatase-phase TiO_2 photocatalyst displayed type IV isotherm, in conjunction with hysteresis loop in the of 0.4 to 1 P/P_0. The surface area of pure anatase-phase TiO_2 was calculated using the Brunnauer–Emmett–Teller (BET) method, with a value of 20 m^2/g. Furthermore, Photocatalyst made of pure anatase-phase TiO_2 exhibits a mesopore size distribution of 38 to 40.7 nm.

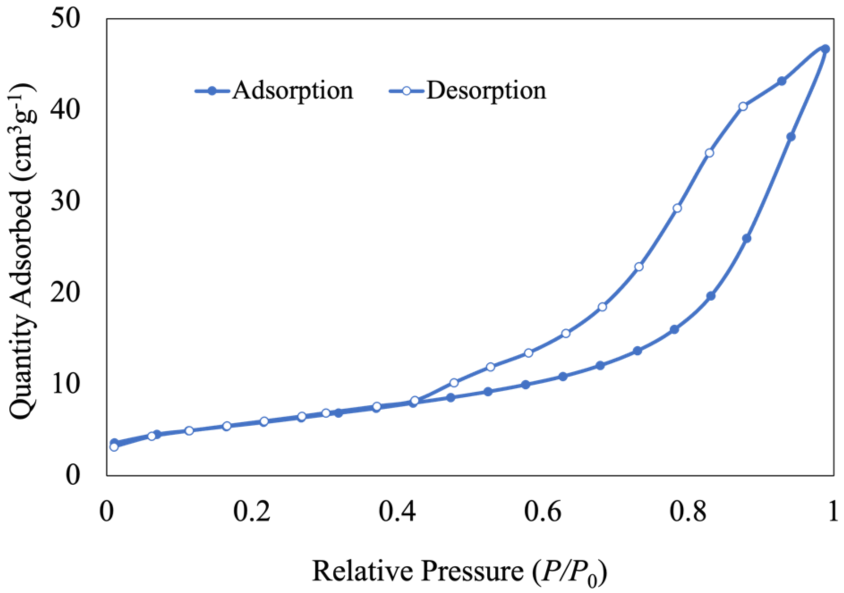

Figure 9: N_2 adsorption–desorption isotherm of pure anatase-phase TiO_2

3.5.4 Scanning Electron Microscopy (SEM) and Energy-Dispersive X-Ray Spectroscopy (EDX) Analyses

Surface morphology of pure anatase-phase TiO_2 exhibited cracked long rod like structure (Figure 10). Moreover, The EDX analysis (Figure 11, Table 2) has confirmed the existence of the elements: Ti, O, in the sample.

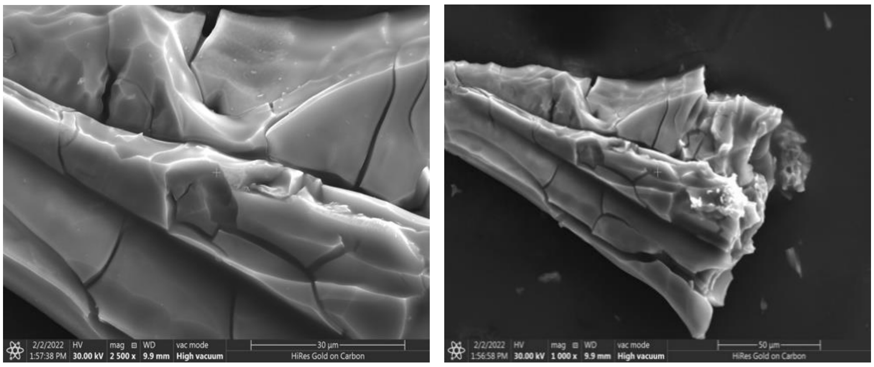

Figure 10: SEM images of pure anatase-phase TiO_2

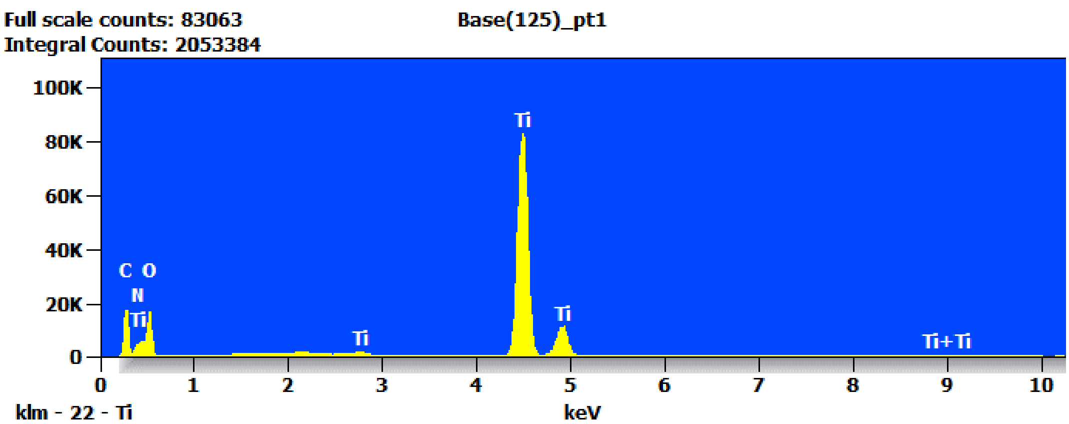

Figure 11: EDX elemental analysis of pure anatase-phase TiO_2

Table 2: Weight and atomic percentages of pure anatase-phase TiO_2

Element	Weight %				Atomic %			
	C	N	O	Ti	C	N	O	Ti
TiO_2	9.22	4.74	41.35	44.7	16.6	7.32	55.9	20.19

3.5.5 Photocatalytic Activities Pure Anatase-Phase TiO_2

To investigate the photocatalytic performance of pure anatase-phase TiO_2 photocatalyst, the photocatalytic cycloaddition of CO_2 to propylene oxide model photocatalytic reaction was undertaken. Based on the integration of ^{1}H-NMR signals, the conversion percent yields of propylene carbonate were calculated as follows:

$$Conversion = \frac{1_{Hb}}{(1_{Ha}+1_{Hb})} \quad (1)$$

In Equation 1, the OCH protons in the starting material (^1H_a) were compared to their respective counterparts in the product (^1H_b) in order to calculate percent conversion (Table 3).

Table 3: The chemical shift of OCH protons of epoxides and the corresponding cyclic carbonates and their yields

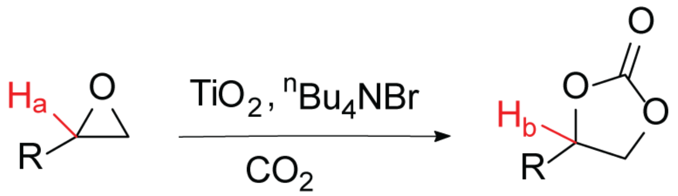

Epoxide	$^{\delta}H_a$ ($CDCl_3$) (epoxide, ^1H_a)	$^{\delta}H_b$ ($CDCl_3$) (carbonate, ^1H_b)	Conversion yield (%)	TON[c]	TOF(h^{-1})[d]
1a	2.98	4.85	99.9	59.54	2.48
1b	3.83	5.65	99.9	59.54	2.48
1c	3.83	5.65	99.9	59.54	2.48
1e	3.04	4.70	30	17.86	0.744

[a] Reaction conditions: epoxide (1.429 mmol), photocatalyst (10 mg, 0.024mmol), $^nBu_4NBr$ (9 mg, 0.028 mmol) and 0.045 mmol carbon dioxide at 353 K and 24 h.
[b] Yield of isolated product was determined by ^{1}H NMR spectroscopy.
[c]TON= (mmols of product)/ (mmols of catalyst).
[d]TOF = (mmols of product)/ (mmols of catalyst) (reaction time, hour).

propylene oxide (1a), styrene oxide (1b), 2-(4-chlorophenyl) oxirane (1c), and 1,2-epoxy-3-phenoxypropane (1e)

Table 3 shows the proton chemical shifts of the epoxide substrates and the corresponding cyclic carbonates and their yields. Based on the obtained results, TiO_2 has highest photocatalytic activity. Cycloaddition of 1,2-epoxy-2-methylpropane to CO_2 gave the lowest conversion yield of 30%.

As shown in Figure 12, the NMR spectra of the product show the expected peaks without any impurities or starting material except when 1,2-epoxy-3-phenoxypropane was used, indicating that the reaction has been completed quantitatively. Since 1,2-epoxy-3-phenoxypropane is the most sterically hindered epoxides used in this study. Accordingly, we speculate that the reaction may occur inside the mesopore of TiO_2 and not in the surface.

To confirm the role of the pure anatase-phase TiO_2 photocatalyst, three control experiments were performed (Table 4): (1) photocatalytic reaction without light at room temperature (entry I), (II) photocatalytic reaction without pure anatase-phase TiO_2 photocatalyst (entry III), and (III) photocatalytic reaction without light at 353 K (entry II). Cyclic propylene carbonate conversion was only 10% when using $^{n}Bu_4NBr$ without the use pure anatase-phase TiO_2 photocatalyst, and only 3% when using 353 K without light, according to the results. Moreover, in the absence pure anatase-phase TiO_2 reaction yielded only 7%.

Table 4: Photocatalytic control experiments of pure anatase-phase TiO_2

Entry	Photocatalyst	Conversion Yield %
I	pure anatase-phase TiO_2, $^{n}Bu_4NBr$, no light, no heat	7
II	pure anatase-phase TiO_2, $^{n}Bu_4NBr$, heat (353K), no light	3
III	Only $^{n}Bu_4NBr$, no catalyst	10
V	Commercial TiO_2	30

3.6 NMR Spectra

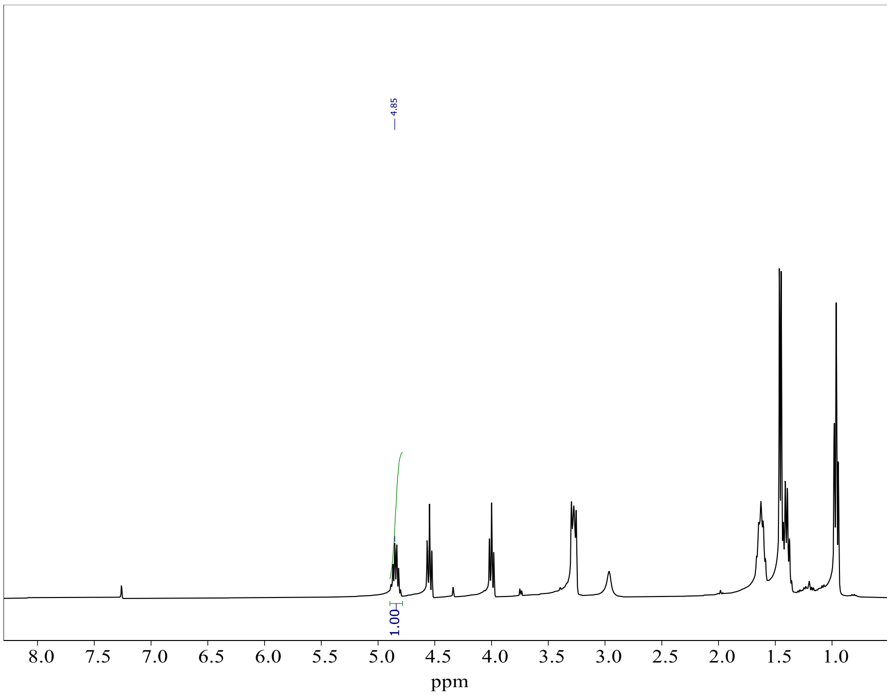

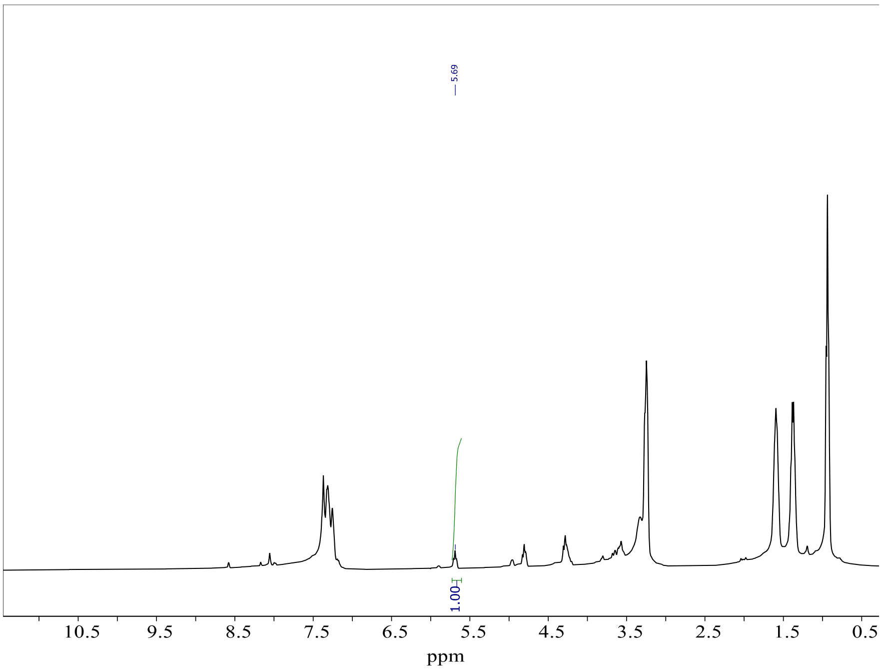

Figure 12: Propylene oxide (1a), styrene oxide (1b), 2-(4-chlorophenyl) oxirane (1c),and 1,2-epoxy-3-phenoxypropane (1e)

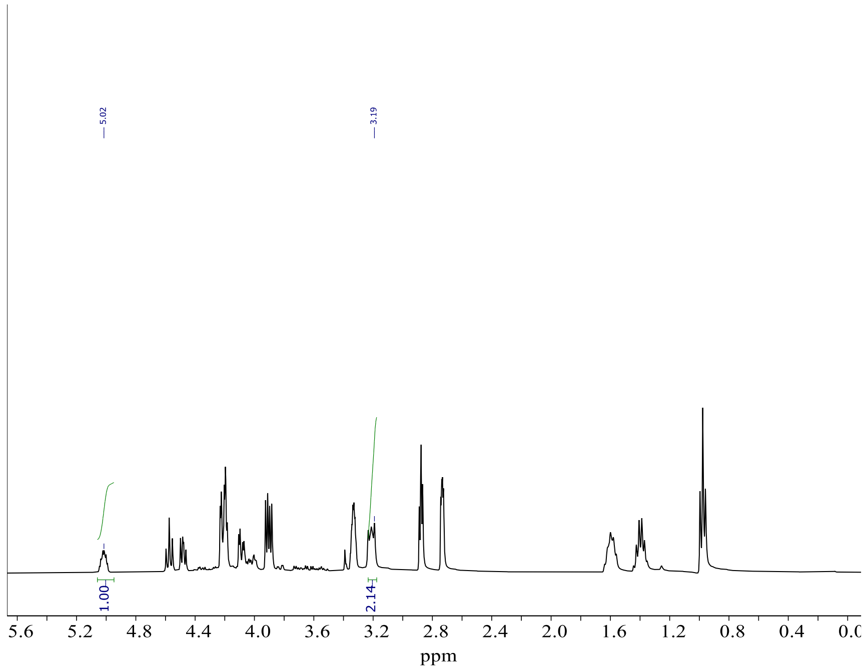

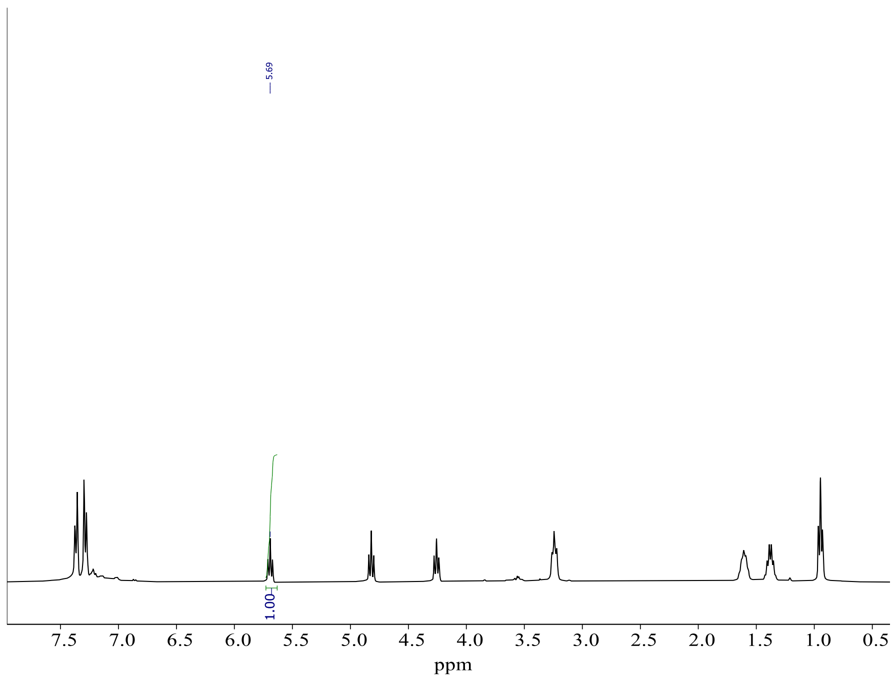

Figure 12: propylene oxide (1a), styrene oxide (1b), 2-(4-chlorophenyl) oxirane (1c),and 1,2-epoxy-3-phenoxypropane (1e) (Continued)

Figure 13 illustrates a plausible mechanism for the photocatalytic CO_2 cycloaddition reaction. The Lewis acidic (Ti^{4+} nodes) sites of prepared pure anatase-phase TiO_2 are expected as the start of a possible mechanism for the CO_2 cycloaddition: the coordination of the oxygen atom from the epoxides weakens the C-O bond. In the next step, A TBAB attacks of the cocatalyst on the C atom of the epoxide then opens the epoxide ring.[67] Finally, cyclic carbonates are formed when activated CO_2 reacts with the C atom of the epoxide (Figure 13).

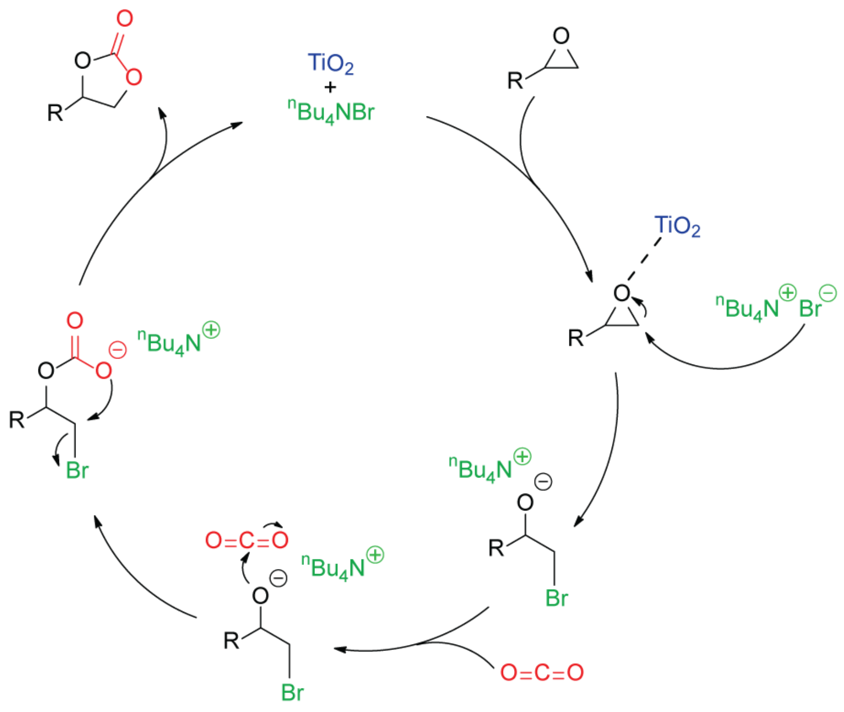

Figure 13: Plausible mechanism for CO_2 cycloaddition of epoxides to cyclic carbonates

3.7 Conclusion

Controlled calcination was used to generate pure anatase-phase TiO_2 photocatalyst using hexanuclear titanium oxo cluster precursor. Pure anatase-phase TiO_2 exhibited band gap value of 3.1 eV allowing it to be used as an active photocatalyst for the CO_2 cycloaddition reaction of epoxides to cyclic carbonates. PXRD pattern of calcined hexanuclear titanium oxo cluster confirm the presence of Pure anatase-phase TiO_2. Prepared TiO_2 was used as an effective photocatalyst for CO_2 cycloaddition to epoxides producing cyclic carbonates quantitatively except when bulky 1,2-epoxy-3-phenoxypropane was used. In conclusion, calcination of titanium oxo cluster provides an easy, and affordable way of producing photoactive catalysts.

Chapter 4: Summary and Future Work

Titanium-Oxo Cluster was used as an active photocatalyst in the CO_2 cycloaddition reaction of epoxides to cyclic carbonate. Diffusion reflectance spectroscopy (DRS), powder X-ray diffraction (PXRD), and scanning electron microscopy were used to investigate the optical properties of the prepared photocatalyst (SEM). As a model photocatalytic cycloaddition reaction of CO_2 to epoxides, hexanuclear titanium oxo cluster demonstrated a high conversion rate to the formation of cyclic carbonates. Furthermore, we demonstrate the successful synthesis of active TiO_2 photocatalysts with hexanuclear titanium oxo cluster as a sacrificial agent. The formation of pure anatase was confirmed by PXRD patterns of calcined titanium oxo cluster photocatalysts. TiO_2 was used as an active photocatalyst in a CO_2 cycloaddition reaction to propylene oxide, which yielded quantitative propylene carbonate. Calcination of hexanuclear titanium oxo clusters is a simple, dependable, and cost-effective method for producing photoactive catalysts for a wide range of photocatalytic reactions.

References

(1) Nasr, M.; Eid, C.; Habchi, R.; Miele, P.; Bechelany, M. Recent Progress on Titanium Dioxide Nanomaterials for Photocatalytic Applications. *ChemSusChem* 2018, *11* (18), 3023–3047.

(2) Li, Q.; Li, X.; Wageh, S.; Al-Ghamdi, A. A.; Yu, J. CdS/Graphene Nanocomposite Photocatalysts. *Adv. Energy Mater.* 2015, *5* (14), 1–28.

(3) Rota Martir, D.; Zysman-Colman, E. Supramolecular Iridium(III) Assemblies. *Coord. Chem. Rev.* 2018, *364*, 86–117.

(4) Wang, S.; Wang, Y.; Zang, S. Q.; Lou, X. W. Hierarchical Hollow Heterostructures for Photocatalytic CO_2 Reduction and Water Splitting. *Small Methods* 2020, *4* (1), 1–11.

(5) Ijaz, M.; Zafar, M. Titanium Dioxide Nanostructures as Efficient Photocatalyst: Progress, challenges and perspective. *International Journal of Energy Research* 2021, *45* (3), 3569-3589.

(6) Chaki Borrás, M.; Sluyter, R.; Barker, P. J.; Konstantinov, K.; Bakand, S. Y2O3 Decorated TiO_2 Nanoparticles: Enhanced UV Attenuation and Suppressed Photocatalytic Activity with Promise for Cosmetic and Sunscreen Applications. *J. Photochem. Photobiol. B Biol.* 2020, *207* (43), 1883–1896.

(7) Nakata, K.; Fujishima, A. TiO_2 Photocatalysis: Design and Applications. *J. Photochem. Photobiol. C Photochem. Rev.* 2012, *13* (3), 169–189.

(8) Jiang, Z.; Hu, J.; Zhang, X.; Zhao, Y.; Fan, X.; Zhong, S.; Zhang, H.; Yu, X. A Generalized Predictive Model for TiO_2–Catalyzed Photo-Degradation Rate Constants of Water Contaminants through Artificial Neural Network. *Environ. Res.* 2020, *187* (5), 109–116.

(9) Kubiak, A.; Bielan, Z.; Bartkowiak, A.; Gabała, E.; Piasecki, A.; Zalas, M.; Zielińska-Jurek, A.; Janczarek, M.; Siwińska-Ciesielczyk, K.; Jesionowski, T. Synthesis of Titanium Dioxide via Surfactantassisted Microwave Method for Photocatalytic and Dye-Sensitized Solar Cells Applications. *Catalysts* 2020, *10* (5), 53–68.

(10) Wang, L.; Huang, X.; Han, M.; Lyu, L.; Li, T.; Gao, Y.; Zeng, Q.; Hu, C. Efficient Inhibition of Photogenerated Electron-Hole Recombination through Persulfate Activation and Dual-Pathway Degradation of Micropollutants over Iron Molybdate. *Appl. Catal. B Environ.* 2019, *257* (12), 117–125.

(11) You, Y.; Tong, X.; Wang, W.; Sun, J.; Yu, P.; Ji, H.; Niu, X.; Wang, Z. M. Eco-Friendly Colloidal Quantum Dot-Based Luminescent Solar Concentrators. *Adv. Sci.* 2019, *6* (9), 24–38.

(12) Suwannaruang, T.; Kamonsuangkasem, K.; Kidkhunthod, P.; Chirawatkul, P.; Saiyasombat, C.; Chanlek, N.; Wantala, K. Influence of Nitrogen Content Levels on Structural Properties and Photocatalytic Activities of Nanorice-like N-Doped TiO_2 with Various Calcination Temperatures. *Mater. Res. Bull.* 2018, *105* (67), 265–276.

(13) Shan, A. Y.; Ghazi, T. I. M.; Rashid, S. A. Immobilisation of Titanium Dioxide onto Supporting Materials in Heterogeneous Photocatalysis: A Review. *Appl. Catal. A Gen.* 2010, *389* (2), 1–8.

(14) Gupta, T.; Samriti; Cho, J.; Prakash, J. Hydrothermal Synthesis of TiO_2 Nanorods: Formation Chemistry, Growth Mechanism, and Tailoring of Surface Properties for Photocatalytic Activities. *Mater. Today Chem.* 2021, *20*, 1004–1016.

(15) Mohammadi, M. R.; Fray, D. J. Nanostructured TiO_2-CeO_2 Mixed Oxides by an Aqueous Sol-Gel Process: Effect of Ce:Ti Molar Ratio on Physical and Sensing Properties. *Sensors Actuators, B Chem.* 2010, *150* (2), 631–640.

(16) Feinle, A.; Elsaesser, M. S.; Hüsing, N. Sol-Gel Synthesis of Monolithic Materials with Hierarchical Porosity. *Chem. Soc. Rev.* 2016, *45* (12), 3377–3399.

(17) Yan, Y.; Li, C.; Wu, Y.; Gao, J.; Zhang, Q. From Isolated Ti-Oxo Clusters to Infinite Ti-Oxo Chains and Sheets: Recent Advances in Photoactive Ti-Based MOFs. *J. Mater. Chem. A* 2020, *8* (31), 15245–15270.

(18) Hong, K.; Chun, H. Nonporous Titanium-Oxo Molecular Clusters That Reversibly and Selectively Adsorb Carbon Dioxide. *Inorg. Chem.* 2013, *52* (17), 9705–9707.

(19) Grignard, B.; Gennen, S.; Jérôme, C.; Kleij, A. W.; Detrembleur, C. Advances in the Use of CO_2 as a Renewable Feedstock for the Synthesis of Polymers. *Chem. Soc. Rev.* 2019, *48* (16), 4466–4514.

(20) Lopes, E. J. C.; Ribeiro, A. P. C.; Martins, L. M. D. R. S. New Trends in the Conversion of CO_2 to Cyclic Carbonates. *Catalysts* 2020, *10* (5), 42–58.

(21) Su, C. C.; He, M.; Amine, R.; Chen, Z.; Sahore, R.; Dietz Rago, N.; Amine, K. Cyclic Carbonate for Highly Stable Cycling of High Voltage Lithium Metal Batteries. *Energy Storage Mater.* 2019, *17* (8), 284–292.

(22) Voropaeva, D. Y.; Novikova, S. A.; Kulova, T. L.; Yaroslavtsev, A. B. Solvation and Sodium Conductivity of Nonaqueous Polymer Electrolytes Based on Nafion-117 Membranes and Polar Aprotic Solvents. *Solid State Ionics* 2018, *324* (27), 28–32.

(23) Rehman, A.; Saleem, F.; Javed, F.; Ikhlaq, A.; Ahmad, S. W.; Harvey, A. Recent Advances in the Synthesis of Cyclic Carbonates via CO_2 cycloaddition to Epoxides. *J. Environ. Chem. Eng.* 2021, *9* (2), 105–113.

(24) Yu, W.; Maynard, E.; Chiaradia, V.; Arno, M. C.; Dove, A. P. Aliphatic Polycarbonates from Cyclic Carbonate Monomers and Their Application as Biomaterials. *Chem. Rev.* 2021, *121* (18), 10865–10907.

(25) Muniandy, L.; Adam, F.; Rahman, N. R. A.; Ng, E. P. Highly Selective Synthesis of Cyclic Carbonates via Solvent Free Cycloaddition of CO_2 and Epoxides Using Ionic Liquid Grafted on Rice Husk Derived MCM-41. *Inorg. Chem. Commun.* 2019, *104* (2), 1–7.

(26) Ma, J.; Song, J.; Liu, H.; Liu, J.; Zhang, Z.; Jiang, T.; Fan, H.; Han, B. One-Pot Conversion of CO_2 and Glycerol to Value-Added Products Using Propylene Oxide as the Coupling Agent. *Green Chem.* 2012, *14* (6), 1743–1748.

(27) Shoaee, S.; Sanna, A. L.; Sforazzini, G. Elucidating Charge Generation in Green-Solvent Processed Organic Solar Cells. *Molecules* 2021, *26* (24), 1–13.

(28) Ahmed, S. N.; Haider, W. Heterogeneous Photocatalysis and Its Potential Applications in Water and Wastewater Treatment: A Review. *Nanotechnology* 2018, *29* (34), 36–47.

(29) Gopinath, K. P.; Madhav, N. V.; Krishnan, A.; Malolan, R.; Rangarajan, G. Present Applications of Titanium Dioxide for the Photocatalytic Removal of Pollutants from Water: A Review. *J. Environ. Manage.* 2020, *270* (4), 110–127.

(30) Belessiotis, G. V.; Kontos, A. G. Plasmonic Silver (Ag)-Based Photocatalysts for H_2 Production and CO_2 Conversion: Review, Analysis and Perspectives. *Renew. Energy* 2022, *195*, 497–515.

(31) Liu, X.; Zhuang, H. Recent Progresses in Photocatalytic Hydrogen Production: Design and Construction of Ni-Based Cocatalysts. *Int. J. Energy Res.* 2021, *45* (2), 1480–1495.

(32) Wei, Z.; Liu, J.; Shangguan, W. A Review on Photocatalysis in Antibiotic Wastewater: Pollutant Degradation and Hydrogen Production. *Chinese J. Catal.* 2020, *41* (10), 1440–1450.

(33) Xu, J.; Huang, L.; He, L.; Ni, Z.; Shen, J.; Li, X.; Chen, K.; Li, W.; Zhang, P. A Combination of Heterogeneous Catalysis and Photocatalysis for the Olefination of Quinoxalin-2(1H)-Ones with Ketones in Water: A Green and Efficient Route to (Z)-Enaminones. *Green Chem.* 2021, *23* (5), 2123–2129.

(34) Das, T. K.; Remanan, S.; Ghosh, S.; Das, N. C. An Environment Friendly Free-Standing Cellulose Membrane Derived for Catalytic Reduction of 4-Nitrophenol: A Sustainable Approach. *J. Environ. Chem. Eng.* 2021, *9* (1), 104–116.

(35) Yu, J.; Dai, G.; Cheng, B. Effect of Crystallization Methods on Morphology and Photocatalytic Activity of Anodized TiO_2 Nanotube Array Films. *J. Phys. Chem. C* 2010, *114* (45), 19378–19385.

(36) Liu, Q. L.; Zhao, Z. Y.; Zhao, R. D.; Yi, J. H. Fundamental Properties of Delafossite $CuFeO_2$ as Photocatalyst for Solar Energy Conversion. *J. Alloys Compd.* 2020, *819*, 153–168.

(37) Li, X.; He, C.; Zuo, S.; Yan, X.; Dai, D.; Zhang, Y.; Yao, C. Photocatalytic Nitrogen Fixation over Fluoride/Attapulgite Nanocomposite: Effect of Upconversion and Fluorine Vacancy. *Sol. Energy* 2019, *191* (57), 251–262.

(38) Wang, Z. L.; Wu, W. Nanotechnology-Enabled Energy Harvesting for Self-Powered Micro-/Nanosystems. *Angew. Chemie - Int. Ed.* 2012, *51* (47), 11700–11721.

(39) Chen, R.; Yan, Z. H.; Kong, X. J. Recent Advances in First-Row Transition Metal Clusters for Photocatalytic Water Splitting. *ChemPhotoChem* 2020, *4* (3), 157–167.

(40) Chen, D.; Cheng, Y.; Zhou, N.; Chen, P.; Wang, Y.; Li, K.; Huo, S.; Cheng, P.; Peng, P.; Zhang, R.; Wang, L.; Liu, H.; Liu, Y.; Ruan, R. Photocatalytic Degradation of Organic Pollutants Using TiO_2-Based Photocatalysts: A Review. *J. Clean. Prod.* 2020, *268*, 1217–1225.

(41) Murillo-Sierra, J. C.; Hernández-Ramírez, A.; Hinojosa-Reyes, L.; Guzmán-Mar, J. L. A Review on the Development of Visible Light-Responsive WO3-Based Photocatalysts for Environmental Applications. *Chem. Eng. J. Adv.* 2021, *5* (3), 43–58.

(42) Theerthagiri, J.; Lee, S. J.; Karuppasamy, K.; Arulmani, S.; Veeralakshmi, S.; Ashokkumar, M.; Choi, M. Y. Application of Advanced Materials in Sonophotocatalytic Processes for the Remediation of Environmental Pollutants. *J. Hazard. Mater.* 2021, *412* (5), 12–28.

(43) Bisaria, K.; Sinha, S.; Singh, R.; Iqbal, H. M. N. Recent Advances in Structural Modifications of Photo-Catalysts for Organic Pollutants Degradation – A Comprehensive Review. *Chemosphere* 2021, *284* (6), 131–142.

(44) MacWan, D. P.; Dave, P. N.; Chaturvedi, S. A Review on Nano-TiO2 Sol-Gel Type Syntheses and Its Applications. *J. Mater. Sci.* 2011, *46* (11), 3669–3686.

(45) Banerjee, A. N. The Design, Fabrication, and Photocatalytic Utility of Nanostructured Semiconductors: Focus on TiO_2-Based Nanostructures. *Nanotechnol. Sci. Appl.* 2011, *4* (1), 35–65.

(46) Chen, T.; Liu, G.; Jin, F.; Wei, M.; Feng, J.; Ma, Y. Mediating Both Valence and Conduction Bands of TiO_2 by Anionic Dopants for Visible- and Infrared-Light Photocatalysis. *Phys. Chem. Chem. Phys.* 2018, *20* (18), 12785–12790.

(47) Kang, X.; Liu, S.; Dai, Z.; He, Y.; Song, X.; Tan, Z. Titanium Dioxide: From Engineering to Applications. *Catalysts* 2019, *9* (43), 73–93.

(48) Aliabadi, B. G.; Gilani, N.; Pasikhani, J. V.; Pirbazari, A. E. Boosting the Photoconversion Efficiency of TiO_2 Nanotubes Using UV Radiation-Assisted Anodization as a Prospective Method: An Efficient Photocatalyst for Eliminating Resistant Organic Pollutants. *Ceram. Int.* 2020, *46* (12), 19942–19951.

(49) Ren, Y.; Han, Y.; Li, Z.; Liu, X.; Zhu, S.; Liang, Y.; Yeung, K. W. K.; Wu, S. Ce and Er Co-Doped TiO2 for Rapid Bacteria- Killing Using Visible Light. *Bioact. Mater.* 2020, *5* (2), 201–209.

(50) Pagáčová, J.; Plško, A.; Papučová, I.; Faturíková, K.; Prnová, A.; Valuchová, J.; Ondrušová, D. Crystallization of TiO2 Xerogel. *J. Therm. Anal. Calorim.* 2020, *142* (5), 1643–1648.

(51) Liu, Y.; Wang, M.; Li, D.; Fang, F.; Huang, W. Engineering Self-Doped Surface Defects of Anatase TiO_2 Nanosheets for Enhanced Photocatalytic Efficiency. *Appl. Surf. Sci.* 2021, *540* (11), 148–163.

(52) Dambournet, D.; Belharouak, I.; Amine, K. Tailored Preparation Methods of TiO_2 Anatase, Rutile, Brookite: Mechanism of Formation and Electrochemical Properties. *Chem. Mater.* 2010, *22* (3), 1173–1179.

(53) Hou, X.; Aitola, K.; Lund, P. D. TiO_2 Nanotubes for Dye-Sensitized Solar Cells—A Review. *Energy Sci. Eng.* 2020, *4*, 1–17.

(54) Mamaghani, A. H.; Haghighat, F.; Lee, C. S. Hydrothermal/Solvothermal Synthesis and Treatment of TiO_2 for Photocatalytic Degradation of Air Pollutants: Preparation, Characterization, Properties, and Performance. *Chemosphere* 2019, *219*, 804–825.

(55) Souza, I. P. A. F.; Crespo, L. H. S.; Spessato, L.; Melo, S. A. R.; Martins, A. F.; Cazetta, A. L.; Almeida, V. C. Optimization of Thermal Conditions of Sol-Gel Method for Synthesis of TiO_2 using RSM and Its Influence on Photodegradation of Tartrazine Yellow Dye. *J. Environ. Chem. Eng.* 2021, *9* (2), 153–172.

(56) Sharma, R.; Sarkar, A.; Jha, R.; Kumar Sharma, A.; Sharma, D. Sol-Gel–Mediated Synthesis of TiO_2 Nanocrystals: Structural, Optical, and Electrochemical Properties. I*nt. J. Appl. Ceram. Technol.* 2020, *17* (3), 1400–1409.

(57) Li, M.; Magdassi, S.; Gao, Y.; Long, Y. Hydrothermal Synthesis of VO2 Polymorphs: Advantages, Challenges and Prospects for the Application of Energy Efficient Smart Windows. *Small* 2017, *13* (36), 1–25.

(58) Morgan, D. L.; Liu, H. W.; Frost, R. L.; Waclawik, E. R. Implications of Precursor Chemistry on the Alkaline Hydrothermal Synthesis of Titania/ Titanate Nanostructures. *J. Phys. Chem. C* 2010, *114* (1), 101–110.

(59) Dawson, W. J. Hydrothermal Synthesis of Advanced Ceramic Powders. *Am. Ceram. Soc. Bull.* 1988, *67* (10), 1673–1678.

(60) Polsongkram, D.; Chamninok, P.; Pukird, S.; Chow, L.; Lupan, O.; Chai, G.; Khallaf, H.; Park, S.; Schulte, A. Effect of Synthesis Conditions on the Growth of ZnO Nanorods via Hydrothermal Method. *Phys. B Condens. Matter* 2008, *403* (20), 3713–3717.

(61) Gupta, S. M.; Tripathi, M. A Review on the Synthesis of TiO_2 Nanoparticles by Solution Route. *Cent. Eur. J. Chem.* 2012, *10* (2), 279–294.

(62) Arconada, N.; Durán, A.; Suárez, S.; Portela, R.; Coronado, J. M.; Sánchez, B.; Castro, Y. Synthesis and Photocatalytic Properties of Dense and Porous TiO_2-Anatase Thin Films Prepared by Sol-Gel. *Appl. Catal. B Environ.* 2009, *86* (12), 1–7.

(63) Schmidt, H. Chemistry of Material Preparation by the Sol-Gel Process. *J. Non. Cryst. Solids* 1988, *100* (3), 51–64.

(64) Nateq, M. H.; Ceccato, R. Sol-Gel Synthesis of TiO_2 Nanocrystalline Particles with Enhanced Surface Area through the Reverse Micelle Approach. *Adv. Mater. Sci. Eng.* 2019, *25*, 63–75.

(65) Tauc, J. Absorption Edge and Internal Electric Fields in Amorphous Semiconductors. *Mater. Res. Bull.* 1970, *5* (8), 721–729.

(66) Li, W.; Liang, R.; Hu, A.; Huang, Z.; Zhou, Y. N. Generation of Oxygen Vacancies in Visible Light Activated One-Dimensional Iodine TiO_2 Photocatalysts. *RSC Adv.* 2014, *4* (70), 36959–36966.

(67) Marciniak, A. A.; Lamb, K. J.; Ozorio, L. P.; Mota, C. J. A.; North, M. Heterogeneous Catalysts for Cyclic Carbonate Synthesis from Carbon Dioxide and Epoxides. *Curr. Opin. Green Sustain. Chem.* 2020, *26*, 100365–100374.

UAE UNIVERSITY MASTER THESIS NO. 2022:78

Titanium dioxide (TiO_2), an important semiconductor, has been used in various applications ranging from sunblock additives to self-cleaning window coatings, antibacterial agents, photovoltaics, and photocatalysis. Due to its photostability, TiO_2 is an extensively used semiconductor photocatalyst in many industries. This thesis represents the synthesis, structure, and photocatalytic activity of TiO_2 (Anatase) photocatalyst, which was prepared using hexanuclear titanium-oxo cluster precursor via temperature-controlled calcination.

Fatmah Alkindi received her MSc in Chemistry from the Department of Chemistry, College of Science at UAE University, UAE. She received her Bachelor in Chemistry from the College of Science, UAE University, UAE.

www.uaeu.ac.ae

Online publication of thesis:
https://scholarworks.uaeu.ac.ae/etds/